Hindawi Publishing Corporation
Journal of Nanomaterials
Volume 2015, Article ID 864864, 6 pages
http://dx.doi.org/10.1155/2015/864864

*Research Article*

# Synthesis of Three-Dimensional $Fe_3O_4$/Graphene Aerogels for the Removal of Arsenic Ions from Water

**Yan Ye,[1] Da Yin,[2] Bin Wang,[2] and Qingwen Zhang[1]**

[1]*College of Petroleum Engineering, China University of Petroleum, Beijing 102249, China*
[2]*Institute of Drilling Engineering, South West Petroleum University, Chengdu 610500, China*

Correspondence should be addressed to Yan Ye; yeyancup@163.com

Received 7 April 2015; Revised 7 June 2015; Accepted 8 June 2015

Academic Editor: William W. Yu



We report the synthesis of three-dimensional $Fe_3O_4$/graphene aerogels (GAs) and their application for the removal of arsenic (As) ions from water. The morphology and properties of $Fe_3O_4$/GAs have been characterized by scanning electron microscopy, transmission electron microscopy, X-ray diffraction, X-ray photoelectron spectroscopy, and superconducting quantum inference device. The 3D nanostructure shows that iron oxide nanoparticles are decorated on graphene with an interconnected network structure. It is found that $Fe_3O_4$/GAs own a capacity of As(V) ions adsorption up to 40.048 mg/g due to their remarkable 3D structure and existence of magnetic $Fe_3O_4$ nanoparticles for separation. The adsorption isotherm matches well with the Langmuir model and kinetic analysis suggests that the adsorption process is pseudo-second-ordered. In addition to the excellent adsorption capability, $Fe_3O_4$/GAs can be easily and effectively separated from water, indicating potential applications in water treatment.

## 1. Introduction

Arsenic's history in science, medicine, and technology has been overshadowed by its notoriety as a poison in homicides. Arsenate and arsenite contaminants in groundwater threaten ecological balance and human health and result in several diseases such as skin or lung cancer [1]. What is worse, with the intensification of human activities, especially mining activities, combustion of fossil fuels has led to more arsenic species pollute groundwater [2]. Thus the remediation of arsenic pollution by way of adsorption has attracted worldwide attention [3–5]. Compared with other adsorbents, magnetic adsorbents such as $Fe_3O_4$ exhibit unique advantages due to their quick and effective magnetic separation [6, 7]. However, the absorption capacity of most synthesized adsorbents and its efficient magnetic separation are difficult to balance as decreasing magnetic particles size enhances adsorption capacity which would undesirably decrease response to an external magnetic field [8, 9].

Graphene, a two-dimensional atomically thick carbon atom arranged in a honeycomb lattice, has attracted much attention for its potential applications in sensors, catalysis, energy-storage devices, and environmental fields because of its excellent electronic, mechanical, and other properties [10–15]. Generally, graphite can be oxidized by strong oxidants and easily exfoliated to the formation of graphene oxide (GO) and reduced graphene oxide (RGO) by reductants. The chemical oxidation modification methods generate plenty of oxygen-containing functional groups in GO and RGO, which offer a potential way to produce large scale of graphene-based materials with a low cost [16]. The unique surface property enables GO as an ideal substrate to anchor inorganic nanoparticles (NPs) for many applications, such as lithium ion battery [17] and water purification [11]. GO is employed as a scaffold for modifying metal oxide nanoparticles to improve their adsorption performance for its lateral dimension up to micrometers and thickness under several nanometers [18–20]. Although GAs supported $Fe_3O_4$ NPs ($Fe_3O_4$/GAs) have been employed for some applications, such as oxygen reduction reaction [21], there are limited reports on the fabrication of $Fe_3O_4$/GAs as absorbent for removing As ions from water up to now.

In this study, 3D $Fe_3O_4$/GAs have been fabricated through hydrothermal method, which have macroporous framework of graphene sheets with uniform deposition of $Fe_3O_4$ NPs. Three-dimensional (3D) graphene aerogels (GAs)

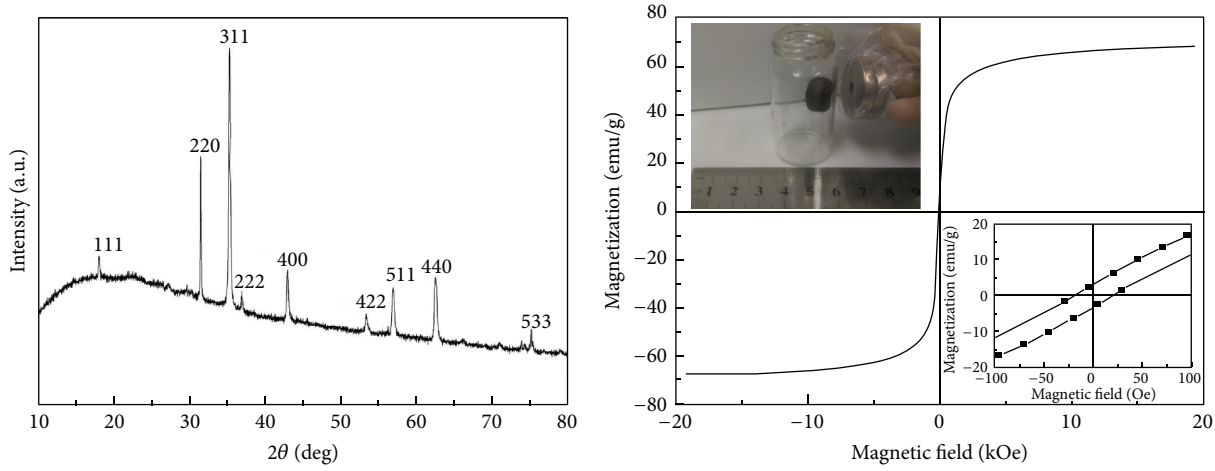


Figure 1: (a) XRD pattern of $Fe_3O_4$/GAs and (b) the magnetization hysteresis loops of $Fe_3O_4$/GAs.

with interconnected mesoporous network, allowing access and diffusion of ions and molecules, seem to be a good candidate as support for iron oxide $Fe_3O_4$ NPs. It was found that $Fe_3O_4$/GAs as self-supported structured adsorbent show excellent capability of removal of As(V) ions in water treatment. Additionally, our results have confirmed that $Fe_3O_4$/GAs can be easily removed from water by magnetic separation.

## 2. Experimental

GO was synthesized using the modified Hummers method [22]. Briefly, 0.5 g of graphite powder and 3 g of potassium permanganate were placed in a 250 mL flask; 60 mL of concentrated sulfuric acid and 6.6 mL of concentrated nitric acid were slowly dropped into the flask under stirring for 12 h at 60°C. Then the mixture was diluted with 0.5 L of deions (DI) water, and excessive 15 mL of hydrogen peroxide (30 wt%) was dumped into the mixture to make bright yellow solution in an ice bath. After repeated centrifugation until neutral (pH = 7) with excessive deionized water (DI), graphite oxide was obtained. Exfoliation of graphite oxide to graphene oxide was achieved by ultrasonication. Then 150 mg of $FeC_2O_4 \cdot 2H_2O$ was added to 35 mL of 2.0 mg·mL$^{-1}$ GO suspension under magnetic stirring for 0.5 h. The stable suspension was sealed in a 50 mL telfon-lined autoclave and hydrothermally treated at 180°C for 12 h and subsequently freeze-dried for 12 h. Finally, after thermal treatment at 600°C for 5 h in Ar gas with 400 sccm, 3D $Fe_3O_4$/GAs were obtained. The structure and surface morphology of $Fe_3O_4$/GAs were investigated by X-ray diffraction (XRD), FEI Quanta 200F scanning electron microscope (SEM), X-ray photoelectron spectroscopy (XPS), and Tecnai G2 F20 transmission electron microscopy (TEM) equipped with selected area electron diffraction (SAED) patterns and scanning TEM (STEM).

The adsorption capability of $Fe_3O_4$/GAs for As(V) ions from water was performed at room temperature. Firstly, individual stock solutions of 1000 mg·L$^{-1}$ and 100 mg·L$^{-1}$ As(V) ions were prepared by dissolving $Na_2HAsO_4 \cdot 7H_2O$ in deionized water, respectively. $Fe_3O_4$/GAs equivalent to 2 mg of aerogels were added into 10 mL of As(V) containing solution with different concentrations (0.50, 1.0, 2.5, 5.0, 10.0, 15.0, 20.0, and 30.0 mg·L$^{-1}$) in the presence of 0.01 M NaCl at a neutral pH. The temperature was maintained at 25°C and the adsorption equilibrium was obtained after 12 h. The remaining concentrations of As(V) ions were magnetically separated by a small magnet and measured by inductively coupled plasma-atomic emission spectroscopy (ICP-AES).

## 3. Results and Discussion

The XRD patterns of $Fe_3O_4$/GAs and GAs are shown in Figure 1(a). The peaks at 2$\theta$ values of 18.9° (111), 31.3° (220), 36.8° (311), 38.5° (222), 44.8° (400), 55.6° (422), 59.3° (511), 65.2° (440), and 77.3° (533) have confirmed the formation of $Fe_3O_4$ (PDF No. 26-1136) in the hybrid [22]. It is worth to note that no apparent diffraction peaks were found between 20° and 30°, indicating that $Fe_3O_4$ NPs have been efficiently deposited on the graphene surface. The magnetic properties of $Fe_3O_4$/GAs were measured using a superconducting quantum inference device with an applied magnetic field of −20000 to 20000 Oe at room temperature. Figure 1(b) shows the curves of magnetization versus applied magnetic field, indicating ferromagnetic behavior of the $Fe_3O_4$/GAs. The saturation magnetization is 68.4 emu/g, which is lower than that of bulk $Fe_3O_4$ (92 emu/g) due to the existence of reduced GO and the small size of $Fe_3O_4$ NPs. The bottom inset in Figure 1(b) shows that the remaining magnetization and coercivity are 3.54 emu/g and 22.6 Oe, respectively. The top inset in Figure 1(b) indicates that the $Fe_3O_4$/GAs have strong responsivity to the external magnetic field, which can be used to separate $Fe_3O_4$/GAs from water.

The typical SEM images (Figures 2(a) and 2(b)) of $Fe_3O_4$/Gas reveal an interconnected porous 3D graphene with continuous macrospores in the micrometer size range, and $Fe_3O_4$ NPs are anchored homogeneously on the graphene

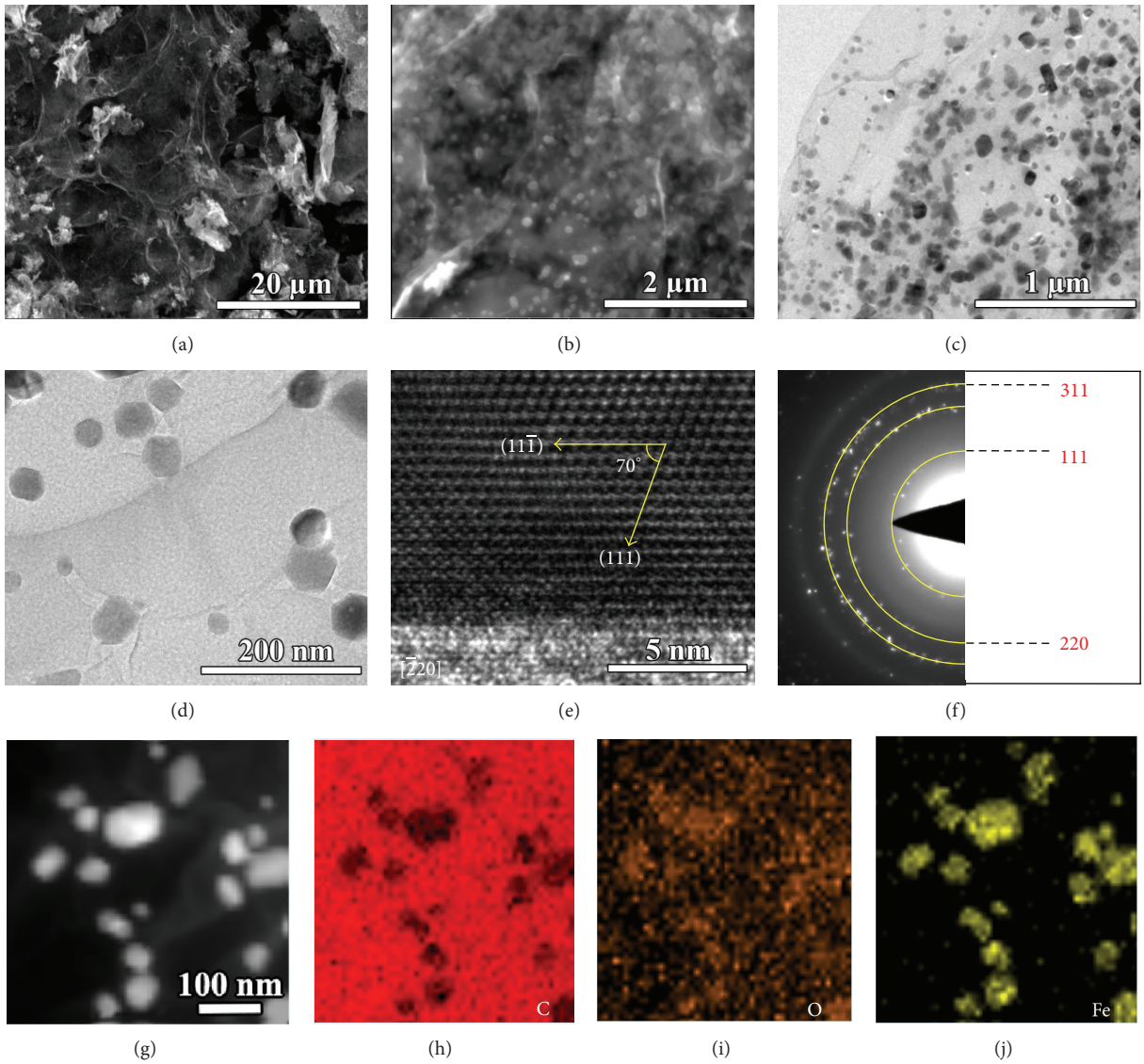


FIGURE 2: (a and b) Typical SEM images of $Fe_3O_4$/GAs, (c and d) TEM images of $Fe_3O_4$/GAs, (e and f) HRTEM and SAED image of $Fe_3O_4$/GAs, and (g–j) STEM elemental mapping of $Fe_3O_4$/GAs.

surface. TEM characterizations (Figures 2(c) and 2(d)) further confirm the uniform distribution of $Fe_3O_4$ NPs on the graphene, and their sizes are in the range of 30~90 nm. High-resolution TEM (HRTEM) image of the hybrid is shown in Figure 2(e) and ED pattern of the NPs further confirms the phases of $Fe_3O_4$ (Figure 2(f)), indicating that well-crystallized $Fe_3O_4$ NPs are tightly formed on the graphene. Moreover, the elemental mapping analysis of $Fe_3O_4$/GAs has confirmed the presence of Fe, O, and C components in the hybrid (Figures 2(g)–2(j)).

Figure 3 shows the XPS pattern of the $Fe_3O_4$/GAs, in which the peaks at 711 eV, 530 eV, and 284 eV are attributed to Fe 2p, O 1s, and C 1s, respectively [22]. In the high-resolution XPS spectrum of Fe 2p (Figure 3(b)), two broad peaks at 725 and 711 eV corresponding to Fe $2p_{1/2}$ and Fe $2p_{3/2}$ were found which are due to the spin orbit splitting [22]. A comparison between the C 1s XPS spectrum of the hybrid (Figure 3(c)) and the C 1s XPS spectrum of GO (top inset in Figure 3(c)) indicates that the GO has been reduced to graphene by ferrous ions during the formation process, due to the significant intensity increase of $sp^2$ C=C bonds of graphene at 284.6 eV and intensity decrease of the oxygen-containing carbon bonds (epoxy C-O at 285.8 eV, carbonyl C=O at 287.3 eV, and carboxyl O=C-O at 289.8 eV [23]). Figure 3(d) shows the O 1s XPS spectrum of the hybrid, which is split into four peaks, and the max peak at 532.2 eV demonstrates the existence of Fe-OH that is favorable to removal of metal irons [14].

The adsorption isotherm of As ions onto $Fe_3O_4$/GAs (Figure 4(a)) shows the relationship between adsorbate and adsorbent. Description on the interaction between adsorption capacity and bond energy, adsorbents, and adsorbates,

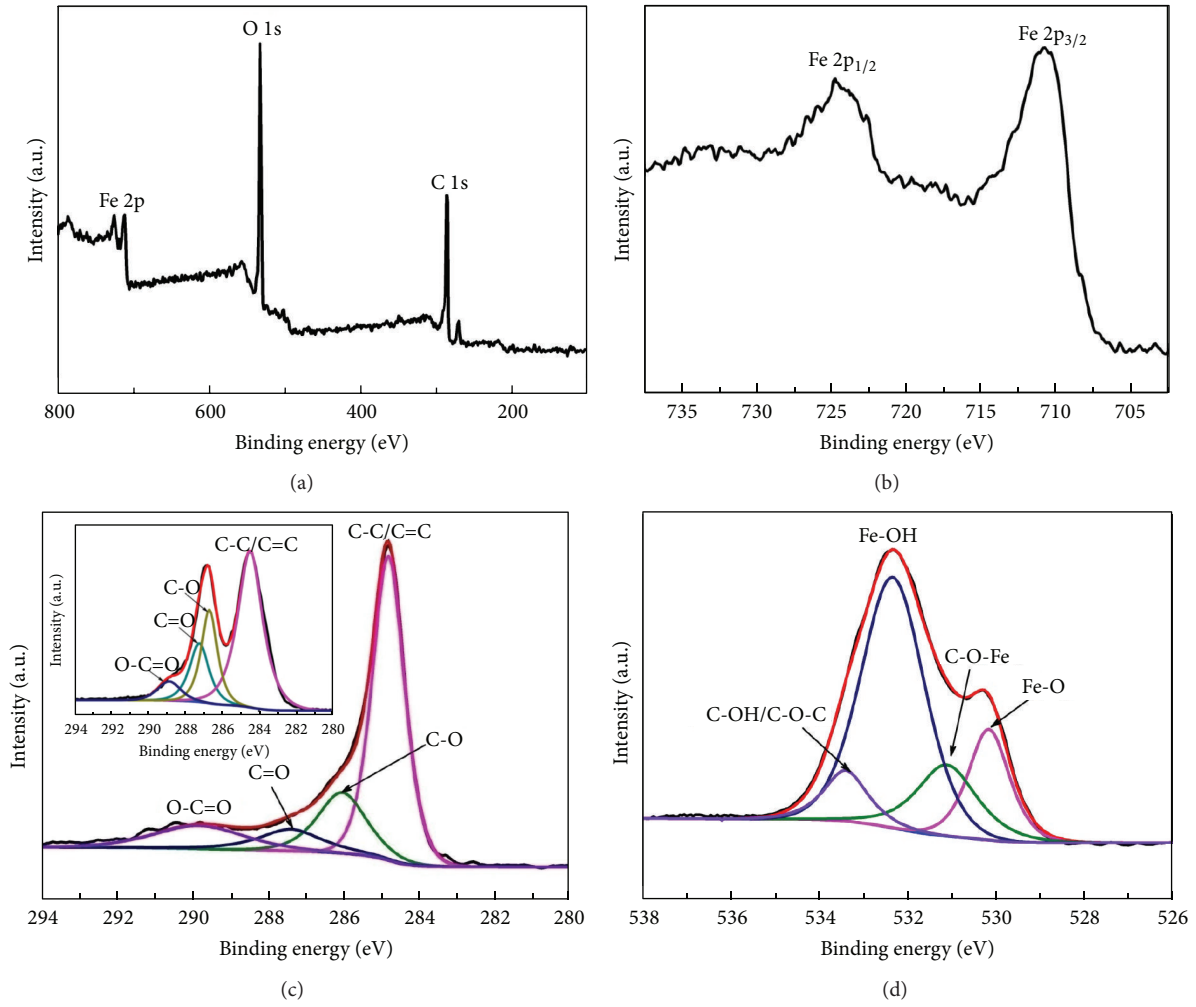


Figure 3: (a) XPS spectrum of $Fe_3O_4$/GAs, (b) a detailed Fe 2p spectrum, (c) a C 1s spectrum of $Fe_3O_4$/GAs and the inset shows a C 1s spectrum of GO, and (d) a O 1s spectrum of $Fe_3O_4$/GAs.

Table 1: Isotherm parameters for removal of As (V).

| Isotherm | Parameters | Values |
|---|---|---|
| Langmuir | $q_m$ (mg/g) | 40.048 |
| | $b$ (L/mg) | 0.124 |
| | $R^2$ | 0.997 |
| Freundlich | $K_F$ (mg/g(L/mg)$^{1/n}$) | 6.479 |
| | $n$ | 1.359 |
| | $R^2$ | 0.982 |

can be determined from isotherm equilibrium models. The experimental data for As ions adsorption have been analyzed by the nonlinear forms of the Langmuir [24] (Figure 4(b)) and Freundlich [25] (Figure 4(c)) isotherm models. The Langmuir model can be expressed as

$$Q_e = \frac{q_m b C_e}{1 + bC_e}. \quad (1)$$

The Freundlich model is given as follows:

$$Q_e = K_F C_e^{1/n}, \quad (2)$$

where $Q_e$ (mg·g$^{-1}$) is the amount adsorbed at equilibrium and $C_e$ (mg·L$^{-1}$) is the equilibrium concentration of adsorbate. The Langmuir constant $q_m$ (mg·g$^{-1}$) represents the maximum adsorption capacity and $b$ (L·mg$^{-1}$) is related to the energy of adsorption. The Freundlich constant ($K_F$) is the parameter and ($1/n$) is the adsorption intensity ($1 < n < 10$). The values of parameters from these isotherm models are listed in Table 1.

The values of correlation coefficient $R^2$ for the Langmuir (0.997) and Freundlich (0.982) models suggest that the adsorption data fit well with the Langmuir model. The maximum adsorption capacity ($q_m$) and $b$ are 40.048 mg·g$^{-1}$ and 0.124 L·mg$^{-1}$, respectively. The adsorption capacity of $Fe_3O_4$/GAs ($q_m$) is larger than that of porous $Fe_3O_4$ particles [26], magnetite-reduced GO composites [11], and other iron-graphene hybrids [27]. The $n$ value is 1.359 in Freundlich mode, which indicates a favorable condition for adsorption.

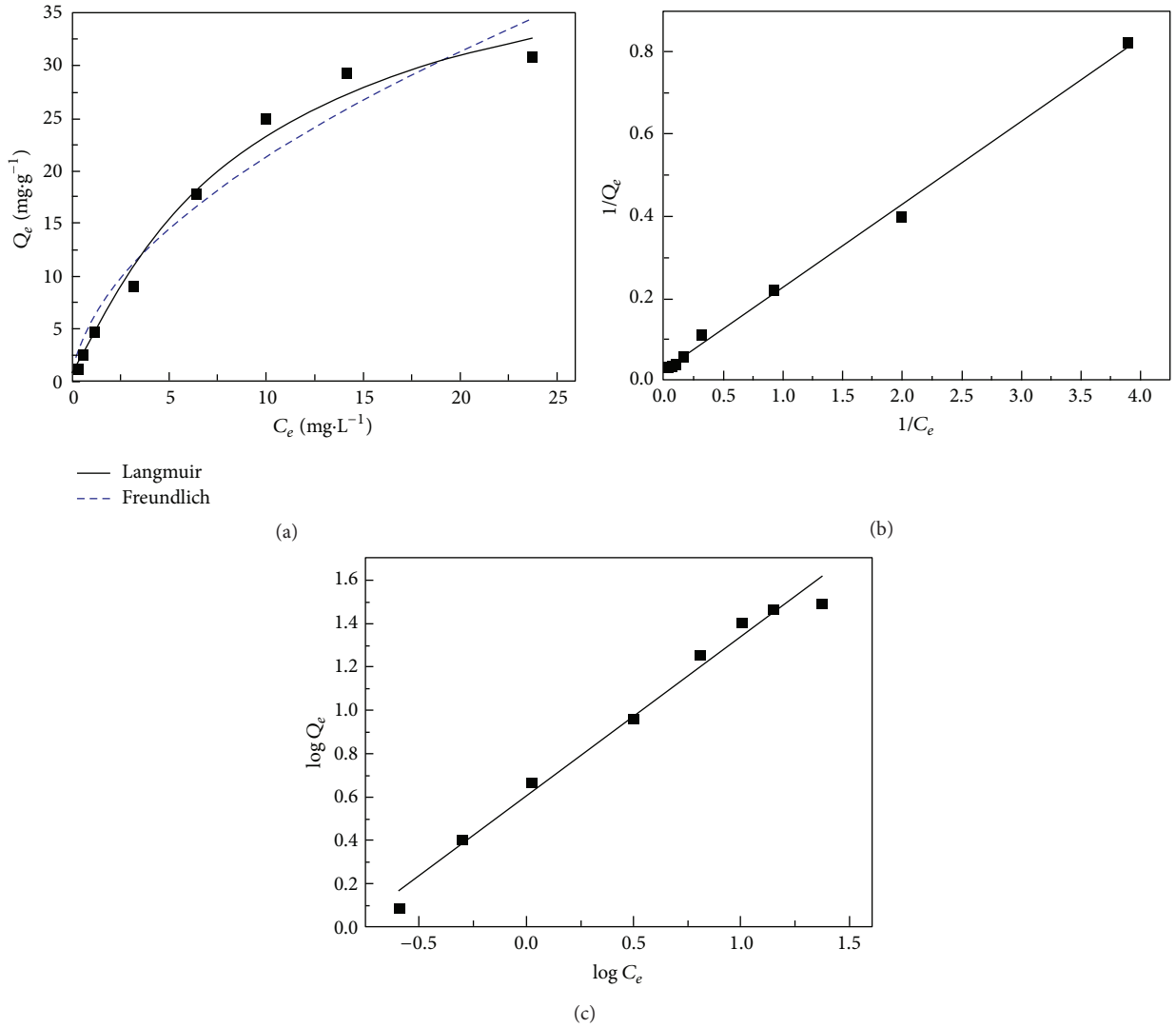


Figure 4: (a) Adsorption isotherm of As on $Fe_3O_4$/GAs at room temperature, (b) Langmuir model, and (c) Freundlich model.

Considering that the adsorbent is environmental friendly and easily to be separated, $Fe_3O_4$/GAs can serve as a more efficient adsorbent in drinking water treatment in the future.

## 4. Conclusion

In summary, 3D $Fe_3O_4$/GAs have been fabricated by a combined method including hydrothermal reaction, freeze-drying, and thermal treatment process. Owing to their 3D macroporous structure, the as-prepared $Fe_3O_4$/GAs have demonstrated excellent adsorptive property of 40.048 mg/g for removing As(V) ions from water and can be easily removed from water. It is believed that the present magnetic $Fe_3O_4$/GAs can be used for more applications, such as catalysis, sensors, and batteries.

## Conflict of Interests

The authors declare that there is no conflict of interests regarding the publication of this paper.

## References

[1] D. Mohan and C. U. Pittman, "Arsenic removal from water/wastewater using adsorbents—a critical review," *Journal of Hazardous Materials*, vol. 142, no. 1-2, pp. 1–53, 2007.

[2] R. Stone, "Arsenic and paddy rice: a neglected cancer risk?" *Science*, vol. 321, no. 5886, pp. 184–185, 2008.

[3] L. Rodríguez-Lado, G. Sun, M. Berg et al., "Groundwater arsenic contamination throughout China," *Science*, vol. 341, no. 6148, pp. 866–868, 2013.

[4] B. Booth, "Cancer rates attributable to arsenic in rice vary globally," *Environmental Science & Technology*, vol. 43, no. 5, pp. 1243–1244, 2009.

[5] C. Baowei, N. Hua, L. Meiling, and X. C. Le, "Metabolism, toxicity, and biomonitoring of arsenic species," *Progress in Chemistry*, vol. 21, no. 2-3, pp. 474–482, 2009.

[6] Z. Ai, Z. Gao, L. Zhang, W. He, and J. J. Yin, "Core-shell structure dependent reactivity of Fe@$Fe_2O_3$ nanowires on aerobic degradation of 4-chlorophenol," *Environmental Science & Technology*, vol. 47, no. 10, pp. 5344–5352, 2013.

[7] W. Yang, A. T. Kan, W. Chen, and M. B. Tomson, "pH-dependent effect of zinc on arsenic adsorption to magnetite nanoparticles," *Water Research*, vol. 44, no. 19, pp. 5693–5701, 2010.

[8] C. T. Yavuz, J. T. Mayo, W. W. Yu et al., "Low-field magnetic separation of monodisperse $Fe_3O_4$ nanocrystals," *Science*, vol. 314, no. 5801, pp. 964–967, 2006.

[9] R. Prucek, J. Tuček, J. Kolařík et al., "Ferrate(VI)-induced arsenite and arsenate removal by in situ structural incorporation into magnetic iron(III) oxide nanoparticles," *Environmental Science & Technology*, vol. 47, no. 7, pp. 3283–3292, 2013.

[10] K. S. Novoselov, A. K. Geim, S. V. Morozov et al., "Electric field effect in atomically thin carbon films," *Science*, vol. 306, no. 5696, pp. 666–669, 2004.

[11] V. Chandra, J. Park, Y. Chun, J. W. Lee, I.-C. Hwang, and K. S. Kim, "Water-dispersible magnetite-reduced graphene oxide composites for arsenic removal," *ACS Nano*, vol. 4, no. 7, pp. 3979–3986, 2010.

[12] Y. Wang, R. Yang, Z. W. Shi et al., "Super-elastic graphene ripples for flexible strain sensors," *ACS Nano*, vol. 5, no. 5, pp. 3645–3650, 2011.

[13] Y. G. Li, H. L. Wang, L. M. Xie, Y. Y. Liang, G. S. Hong, and H. J. Dai, "$MoS_2$ nanoparticles grown on graphene: an advanced catalyst for the hydrogen evolution reaction," *Journal of the American Chemical Society*, vol. 133, no. 19, pp. 7296–7299, 2011.

[14] L. Li, G. M. Zhou, Z. Weng, X.-Y. Shan, F. Li, and H.-M. Cheng, "Monolithic $Fe_2O_3$/graphene hybrid for highly efficient lithium storage and arsenic removal," *Carbon*, vol. 67, pp. 500–507, 2014.

[15] Y. Yao, S. Miao, S. Liu, L. P. Ma, H. Sun, and S. Wang, "Synthesis, characterization, and adsorption properties of magnetic $Fe_3O_4$@graphene nanocomposite," *Chemical Engineering Journal*, vol. 184, pp. 326–332, 2012.

[16] G. M. Scheuermann, L. Rumi, P. Steurer, W. Bannwarth, and R. Mülhaupt, "Palladium nanoparticles on graphite oxide and its functionalized graphene derivatives as highly active catalysts for the Suzuki-Miyaura coupling reaction," *Journal of the American Chemical Society*, vol. 131, no. 23, pp. 8262–8270, 2009.

[17] A. Bhaskar, M. Deepa, T. N. Rao, and U. V. Varadaraju, "Enhanced nanoscale conduction capability of a $MoO_2$/Graphene composite for high performance anodes in lithium ion batteries," *Journal of Power Sources*, vol. 216, pp. 169–178, 2012.

[18] H. Wang, X. Yuan, Y. Wu et al., "Graphene-based materials: fabrication, characterization and application for the decontamination of wastewater and wastegas and hydrogen storage/generation," *Advances in Colloid and Interface Science*, vol. 195-196, pp. 19–40, 2013.

[19] S. Vadahanambi, S.-H. Lee, W.-J. Kim, and I.-K. Oh, "Arsenic removal from contaminated water using three-dimensional graphene-carbon nanotube-iron oxide nanostructures," *Environmental Science & Technology*, vol. 47, no. 18, pp. 10510–10517, 2013.

[20] K. Zhang, V. Dwivedi, C. Chi, and J. Wu, "Graphene oxide/ferric hydroxide composites for efficient arsenate removal from drinking water," *Journal of Hazardous Materials*, vol. 182, no. 1, pp. 162–168, 2010.

[21] Z.-S. Wu, S. Yang, Y. Sun, K. Parvez, X. Feng, and K. Müllen, "3D nitrogen-doped graphene aerogel-supported $Fe_3O_4$ nanoparticles as efficient electrocatalysts for the oxygen reduction reaction," *Journal of the American Chemical Society*, vol. 134, no. 22, pp. 9082–9085, 2012.

[22] W. F. Chen, S. R. Li, C. H. Chen, and L. F. Yan, "Self-assembly and embedding of nanoparticles by in situ reduced graphene for preparation of a 3D graphene/nanoparticle aerogel," *Advanced Materials*, vol. 23, no. 47, pp. 5679–5683, 2011.

[23] H.-J. Shin, K. K. Kim, A. Benayad et al., "Efficient reduction of graphite oxide by sodium borohydride and its effect on electrical conductance," *Advanced Functional Materials*, vol. 19, no. 12, pp. 1987–1992, 2009.

[24] I. Langmuir, "The adsorption of gases on plane surfaces of glass, mica and platinum," *The Journal of the American Chemical Society*, vol. 40, no. 9, pp. 1361–1403, 1918.

[25] H. Freundlich, *Ueber die Adsorption in Loesungen*, Engelmann, Leipzig, Germany, 1906.

[26] T. Wang, L. Y. Zhang, H. Y. Wang et al., "Controllable synthesis of hierarchical porous $Fe_3O_4$ particles mediated by poly (diallyldimethylammonium chloride) and their application in arsenic removal," *ACS Applied Materials & Interfaces*, vol. 5, no. 23, pp. 12449–12459, 2013.

[27] C. Wang, H. J. Luo, Z. L. Zhang, Y. Wu, J. Zhang, and S. W. Chen, "Removal of As(III) and As(V) from aqueous solutions using nanoscale zero valent iron-reduced graphite oxide modified composites," *Journal of Hazardous Materials*, vol. 268, pp. 124–131, 2014.